Shear zones in granular materials: Optimization in a self-organized random potential

J. Török,[1,2] T. Unger,[2] J. Kertész,[2] and D. E. Wolf[3]
[1]*Department of Chemical Information Technology, Budapest University of Technology and Economics, H-1111 Budapest, Hungary*
[2]*Department of Theoretical Physics, Budapest University of Technology and Economics, H-1111 Budapest, Hungary*
[3]*Department of Physics, University Duisburg-Essen, D-47048 Duisburg, Germany*
(Received 15 March 2006; published 25 January 2007)

We introduce a model to describe the wide shear zones observed in modified Couette cell experiments with granular material. The model is a generalization of the recently proposed approach based on a variational principle. The instantaneous shear band is identified with the surface that minimizes the dissipation in a random potential that is biased by the local velocity difference and pressure. The apparent shear zone is the ensemble average of the instantaneous shear bands. The numerical simulation of this model matches excellently with experiments and has measurable predictions.

DOI: 10.1103/PhysRevE.75.011305 PACS number(s): 45.70.−n, 83.50.Ax

Strain localization or shear band formation in granular materials has been studied for many years [1,2] due to its importance in engineering and geoscience. *Shear bands* are narrow regions separating almost solid blocks moving with different velocities. Recently Fenistein and co-workers observed [3,4] wide *shear zones* in a modified cylindrical Couette cell. Instead of letting an inner cylinder rotate with respect to an outer one, their cell has no inner wall, but exerts the shear deformation via the bottom, which is split into a rotating inner disk of radius R_s and a fixed outer annulus (see Fig. 1). The shear zone is pinned at the bottom split and evolves independently of walls. This approach has attracted considerable interest [5–7] because it provides new insight into the fundamental problem of shear band formation.

A theory based on the principle of minimum dissipation rate was proposed soon after the first publications. With the assumption of negligible width of the shear zone a model with no fitting parameter resulted which was used to describe the position of the shear zones [5]. This model proved to be efficient and even delivered predictions about a new type of closed shear zones, which were found later both in experiments and in computer simulations [6,7]. However, the model has to be generalized in order to describe the interesting phenomena related to the width of the shear zone, and this is the aim of the present paper.

Let us first briefly summarize the experimental findings: The shear zone starts from the bottom split, and for small and moderate filling $H \lesssim 0.7R_s$ it ends up on the surface [3]. If the filling height is further increased, the shear zone is buried in the material and takes the shape of a cupola [5–7]. The surface position of the shear zone for small filling can be very well described by a universal empirical curve. The width of the shear zones on the surface increases as a power law with the filling height with an exponent $\sim 2/3$. For the shape and width of closed shear zones, however, there are only qualitative experimental results so far.

Our model combines the ideas of two main sources. The first one is our former theoretical analysis of shear zones based on the principle of minimum dissipation [5]. This narrow band (NB) model assumes that the shear zone is infinitely thin, separating the standing and moving parts of the material. The local dissipation rate is proportional to the velocity difference across the shear band and to the hydrostatic pressure. In this simple model the position of the shear band is identified with the shape that corresponds to the global minimum dissipation rate. By definition, this model was only able to describe the position of the shear band. Due to the cylindrical symmetry, the problem was traced back to finding the minimum path in a smooth two-dimensional (2D) potential. In spite of its simplicity, the model gave surprisingly accurate results; moreover, it predicted the transition from the open [Fig. 1(b)] to the closed [Fig. 1(c)] shapes.

Another optimization problem was introduced earlier in the context of shear band localization during compactification in sheared loose granular matter [8]. In that model instantaneous shear bands were identified by the global mini-

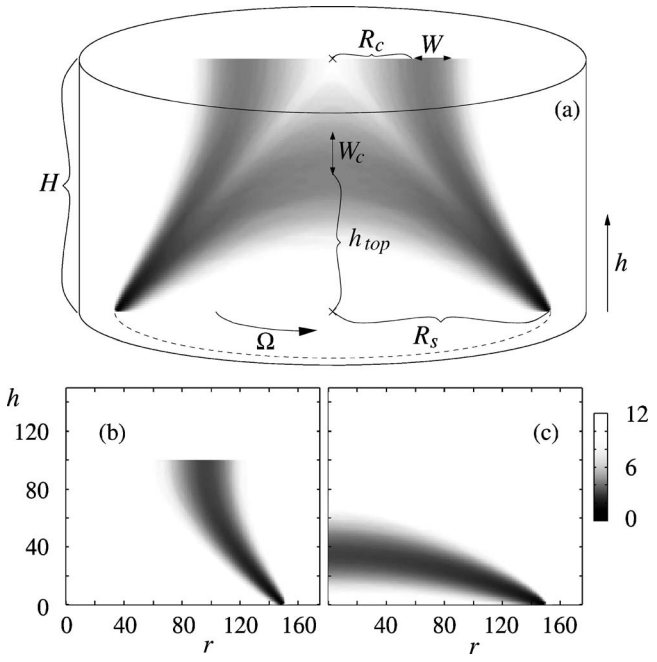

FIG. 1. (a) The experimental arrangement and calculated shear bands. The dotted circle is the bottom split; the definition of the most important quantities are noted in the figure. The gray scaling on all plots is proportional to the logarithm of the occurrence probability at the given point. $R_s = 150$ for (a)–(c) and $H = 115$, 100, and 150 for plots (a), (b), and (c), respectively.

mum of a random potential representing the local inhogeneities of the granular material. These inhogeneities are not frozen in but change due to the relative displacement in the shear band. Thus the global minimum may be at a different place in the next moment, giving rise to an ensamble of instantaneous shear bands which can be associated with the visible macroscopic displacement field. These two models are here combined, and the fluctuations induced by the random potential are used to address the problem of the width of the shear bands.

We generalize the NB model in the following way: Instead of using a smoothly varying potential like in [5] we use a random one which is suited better to the disordered nature of granular media. Like in Ref. [8], the instantaneous displacement is represented by a single localized shear band determined by optimization on a random field: The shear band is the path which minimizes the dissipation rate and obeys the boundary conditions. (We shall again assume that, due to the symmetry of the problem, the determination of the band reduces to that of a line.) The shear is known to change the local structure of the material which we take into account by changing the randomness in the neighborhood of the actual shear band. A new optimal shear band is then searched for. For each random realization of the material the minimization determines a single narrow band. The shear zone itself is represented as an ensemble of narrow bands; i.e., the flow velocity of the material can be obtained as an ensemble average over the realizations. Our approach is related to the first-passage percolation problem [9], also known as a polymer in a random medium [10], though in our case the randomness organizes itself dynamically.

The model is defined on a regular square lattice which is applied as a coarse-grained representation of the material in a radial cut from the center to the outer wall. The shear band is represented by a continuous path that starts from the split point of the bottom and reaches either the surface or the axis of the sample. We allow nearest- and next-nearest-neighbor connections with lengths $\Delta\ell$ equal to 1 and $\sqrt{2}$, respectively. Such a path $\mathcal{P}$ stands for a possible sliding surface with cylindrical symmetry.

The energy dissipation rate associated with path $\mathcal{P}$ is in this geometry proportional to the torque due to the local friction forces. These are modeled by a random strength parameter $u(r,h)$ assigned to each site of the lattice, where r and h are the radial and height coordinates. Each random variable u is generated uniformly in $[\alpha u_{max}, u_{max}]$, $0 \leqslant \alpha \leqslant 1$. As in Ref. [5] we set $u_{max}=r^2(H-h)$, which up to constant factors is hydrostatic pressure $(H-h)$ times cylindrical circumference $(2\pi r)$ times lever (r). The torque is then given by integrating the local shear resistance of the material over the path $\mathcal{P}$: $\mathcal{S}=\Sigma_{i\in\mathcal{P}} u_i \Delta\ell_i$. The actual instantaneous shear band is the directed path [11] that can be activated by the smallest torque—i.e., the one which minimizes $\mathcal{S}$.

Once the minimal path is found, we refresh the strength parameters u randomly along it and in its vicinity (nearest-neighbor-sites). By the successive application of this procedure an ensemble of shear bands is collected which provides the velocity field of the shear flow. One instantaneous shear band separates the sample into two parts in such a way that each site in the inner part rotates by the driving angular velocity Ω of the bottom disk while the sites in the outer part have angular velocity zero. Taking an average over the ensemble of shear bands one arrives at a field of angular velocity that can be compared directly to that observed in experiments.

An important difference between the model of [8] and the present one is that the randomness is refreshed not only on the current minimal path but also in its neighborhood. If only the values in the path were changed, no steady state would be reached. The average value of the randomness u would increase continuously, however extremely slowly. This is not the case here where the steady state is reached fast as in experiments. This variant of the model is closely related to the self-organized criticality model of Bak and Sneppen [12].

The model has three free dimensionless parameters R_s/H, R_s/a, and α: in other words, the aspect ratio of the sample, the split radius in units of the lattice constant, and a number which controls the effect of disorder in the model. We use $a=1$; i.e., all lengths are measured in units of a. The parameter α mimics strength fluctuations due to individual properties (shape, friction, etc.) and cooperative effects (e.g., density fluctuations). Smaller α means stronger disorder, while $\alpha=1$ is a lattice version of the deterministic NB model [13]. We present data for several different values $\alpha=0, 0.43, 0.5, 0.6$ and many different split radii in the range of $R_s=15-600$. As the lattice unit must be larger than the lower length cutoff—i.e., the particle diameter—larger values of R_s correspond to smaller grain size.

In Fig. 1 the probability distribution of instantaneous shear band positions is plotted. We get very similar patterns as the ones obtained in experiments and molecular dynamics simulations [6,7] with both open and closed shear zones. We calculate the angular velocity at any point of the sample and compare it to the experiments.

If the shear zones are far from the system boundaries, the error function is a very good fit for the angular velocity in agreement with the experiments [3]. It gives both the position and width of the zones.

Most of the experimental data concern the surface position of the shear zones (R_c). We compare first this property in Fig. 2(a). The analytical result of [5] overestimated the experiments for $H/R_s \gtrsim 0.25$. Increasing randomness decreases the apparent shear zone radius with the best matching at about $\alpha \simeq 0.5$. System size does not influence the curves for $R_s \gg 10$.

Fenistein and van Hecke [3] suggested a power law dependence of the surface position on the height: namely, $1-R_c/R_s=(H/R_s)^{2.5}$. Thus in Fig. 2(b) we test it on a log-log scale. Both the NB model calculation and our numerical data deviate slightly from the simple power law function for small H/R_s. This deviation is too small to be seen on a normal plot but could be tested in the experiments if high enough precision can be attained [14].

In the experiments the width of the shear zones on the surface was found to be a power law of H with an exponent of 2/3 [6]. Directed polymers have the same roughening exponent [10]. As shown in Fig. 3 we obtain an exponent very close to this value. The curves for different R_s (but the same α) can be scaled together by plotting $W/R_s^{2/3}$ versus H/R_s as in the experiments [6].

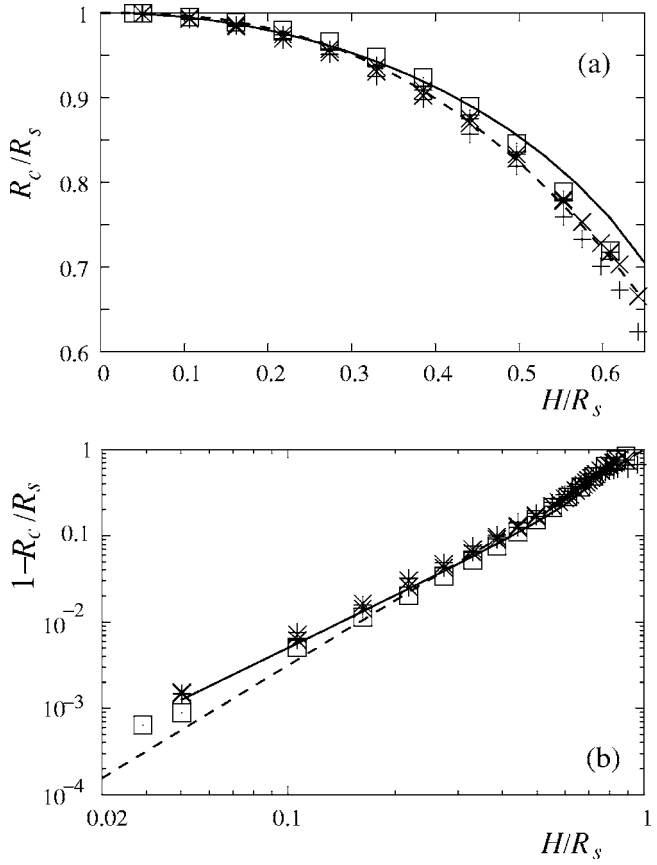

FIG. 2. The surface positions of the shear zones in normal scale (a) and in log-log scale (b). The solid line is from [5]; the dashed line is the experimental [3] curve. Symbols were obtained for systems with R_s=90 and α=0, 0.43, 0.5, and 0.6 for +, ×, ○, and ⊡, respectively.

This power law increase of W with H must stop when the width of the shear zone reaches R_c—i.e., the available distance between the container axis and the average shear band position at the surface. For larger H this finite-size effect

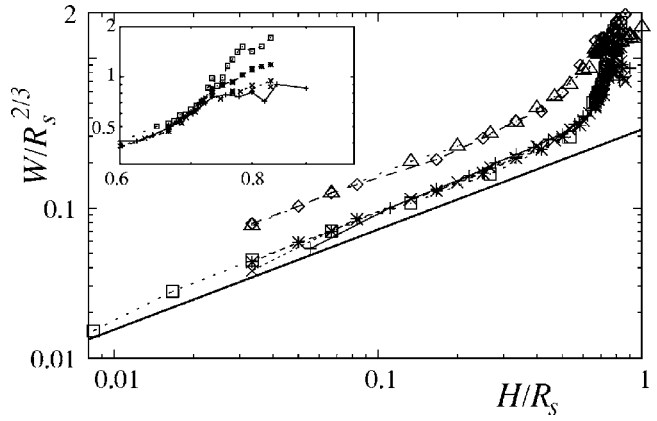

FIG. 3. The surface width of the shear zones. The solid line is $(H/R_s)^{2/3}$. The lower curves are for α=0.43 with R_s=90, 150, 300, and 600 with symbols +, ×, ∗, and ⊡, respectively. The upper curves are for α=0 with R_s=150 and 300 with symbols ◇ and △, respectively. The breakdown of scaling close to the transition is shown in the inset for α=0.43.

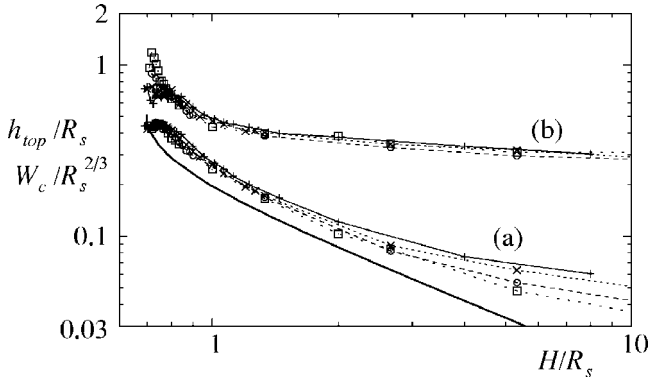

FIG. 4. The scaled center position [curves (a)] and width [curves (b)] of the closed shear zones. The solid line is the calculated position from [5]. Data points (+, ×, ○, ⊡) connected with dashed lines have R_s=90, 150, 300, 600 and α=0.43.

implies that $W \approx R_c \propto R_s$ (for given H/R_s), which explains the sudden increase of W and the loss of data collapse of the scaled curves in Fig. 3 at about $H/R_s \simeq 0.7$, as observed also in the experimental results [6]. It cannot be interpreted as a sign of an increasing characteristic length scale at the transition from open to closed shear zones.

We find that the width of the shear zone depends strongly on α which agrees with experiments where the width is influenced by the shape of the particles. However, the width can also be tuned by the applied resolution of the lattice. Therefore it is not obvious whether the parameter α represents just a rescaling of the lattice constant or is a new, independent parameter which is needed to describe the rheology. The simplest scenario would be that a single intrinsic length l_{eff} suffices to characterize the flow and that particle properties (size, shape, hardness, etc.) enter only through l_{eff}. By contrast our model suggests that an additional disorder parameter has to be included in the description. This second scenario is favored by Fig. 2 where α shifts the surface position R_c while R_c remains unaffected by changing the resolution of the lattice. Although the position shift is small, it might be important because it cannot be explained by a single l_{eff}. An accurate measurement that is able to confirm or reject the existence of this small effect can select the physically relevant scenario.

Due to the occurrence of closed shear zones, the local angular velocity on the symmetry axis of the container depends on h, being equal to Ω at the bottom and decreasing monotoneously towards the surface. By fitting this dependence again by an error function, we determine the position h_{top} and vertical width W_c of the closed shear zones. This works as well as on the surface provided the shear zone is not too close to the boundaries. This fitting procedure has a much broader range of applicability than the one with half a Gaussian which works well only for small systems $R_s \lesssim 30$ with moderate $H \lesssim R_s$ [7].

Some of our measured datasets are plotted in Fig. 4. The closed shear zones become flatter with increasing H. The position scales with R_s and follows the curve calculated in [5] for values of H/R_s between 0.8 and 2. The deviations for

larger H/R_s can be understood by noting that the height of the shear zone decreases faster than the width with increasing H. Above a certain filling height the shear zones touch the bottom of the container. This raises the apparent position of the shear zones compared to the noiseless system of [5].

The vertical width W_c of the closed shear zones scales with $R_s^{2/3}$, as expected for directed polymers with a length of the order R_s. Close to the transition, for H/R_s between 0.7 and 0.8, both W_c and h_{top} deviate from the expected behavior. Again this can be understood as a boundary effect: In the absence of fluctuations, h_{top} is closer to the surface than the width W_c permits.

The next question we focus on is the phase transition. There seems to be a discrepancy between the theoretical model [5] which predicts a first-order transition and the experiments [6,7] which claim to see a continuous transition. The latter two experimental papers introduce different empirical fittings of the shear zone profiles and show the transition of the fitting parameters. Both papers estimate that the transition occurs at lower H/R_S ($H/R_S \simeq 0.6$ [7], $H/R_S \simeq 0.65$ [6]) than in the theory of [5]. The drawback of both approaches is that only one side of the transition can be studied.

We prefer the classical approach of the order parameter of the transition. A good candidate seems to be the normalized angular velocity of the surface at the center, $m \equiv \omega(r=0, h=H)/\Omega$. If the system has only open shear bands, $m=1$, and if only closed ones, $m=0$. If both types are present, m can take any value between 0 and 1.

Figure 5 shows the change of m with H/R_s for different R_s and $\alpha=0$. The transition gets sharper as the system size increases: In the thermodynamic limit $R_s \to \infty$, its width seems to vanish like $R_s^{-1/2}$ (see inset of Fig. 5). Then the order parameter jumps at a value of H/R_s, which we could estimate from a finite-size scaling analysis as $(H/R_s)_c \simeq 0.735$. Remarkably, this is very close to the higher limit of the hysteresis calculated in [5].

The angular velocity of the surface at the center is available in experiments so that the test of the order parameter is straightforward. The plot of m for three systems can be found in Ref. [6]. The experimental results look quite similar but with a little shift in H/R_s. The sharpening of the transition cannot be tested in these experiments due to the limited range of R_s.

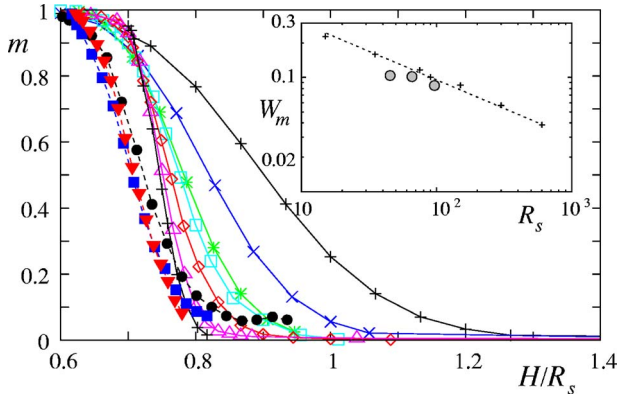

FIG. 5. (Color online) The order parameter m for $\alpha=0$. System size $R_s=15,35,75,90,150,300,600$ from right to left, respectively ($+$, $\times$, $*$, $\boxdot$, $\diamond$, $\triangle$, $+$). Experimental data from [6] are shown with solid symbols of $\odot$, $\triangledown$, and $\boxdot$ for $R_s=45$, 65, and 95 cm, respectively. The inset shows the width of the tranisition versus R_s for $+$ experiments $\odot$. The dashed line has a slope of 0.5.

In conclusion we have shown that the results obtained from numerical simulations of our model can be *directly* compared to the experimental ones. Excellent agreement can be obtained for the already measured quantities such as surface position, width, and angular velocity at the center of the surface. The comparison with experiments shows that our lattice constant can be indentified roughly with a one-particle diameter. This also draws attention to the fact that the experimental systems $R_s=15-95$ are far from the thermodynamic limit especially if one studies the order of the transition.

The variational principle combined with the self-organized random potential turned out to be an efficient tool to study shear zones. Applications to other geometries are straightforward.

We thank M. van Hecke and J.B. Lechman for useful discussions. Support by Grants Nos. OTKA F047259 and T049403, by G.I.F. research Grant No. I-795-166.10/2003, and by the Humboldt Foundation is acknowledged.

[1] *Physics of Dry Granular Media*, edited by H. J. Herrmann, J.-P. Hovi, and S. Luding (Kluwer Academic, Dordrecht, 1998).
[2] H. M. Jaeger, S. R. Nagel, and R. P. Behringer, Rev. Mod. Phys. **68**, 1259 (1996).
[3] D. Fenistein and M. van Hecke, Nature (London) **425**, 256 (2003).
[4] D. Fenistein, J. W. van de Meent, and M. van Hecke, Phys. Rev. Lett. **92**, 094301 (2004).
[5] T. Unger, J. Török, J. Kertész, and D. E. Wolf, Phys. Rev. Lett. **92**, 214301 (2004).
[6] D. Fenistein, J. W. van de Meent, and M. van Hecke, Phys. Rev. Lett. **96**, 118001 (2006).
[7] X. Cheng, J. B. Lechman, A. Fernandez-Barbero, G. S. Grest, H. M. Jaeger, G. S. Karczmar, M. E. Möbius, and S. R. Nagel, Phys. Rev. Lett. **96**, 038001 (2006).
[8] J. Török, S. Krishnamurthy, J. Kertész, and S. Roux, Phys. Rev. Lett. **84**, 3851 (2000).
[9] D. Ben-Avraham and S. Havlin, *Diffusion and Reactions in Fractals and Disordered Systems* (Cambridge University Press, Cambridge, England, 2000).
[10] Y. C. Zhang and T. Halpin-Healy, Phys. Rep. **254**, 215 (1995).
[11] A. Hansen and J. Kertész, Phys. Rev. Lett. **93**, 040601 (2004); Y. Chen, E. López, S. Havlin, and H. E. Stanley, *ibid.* **96**,

068702 (2006).
[12] P. Bak and K. Sneppen, Phys. Rev. Lett. **71**, 4083 (1993).
[13] For $\alpha \gtrsim 0.7$ the lattice geometry has a strong influence on the shape of the shear bands. We restrict ourselves to the range $\alpha \in [0:0.6]$.
[14] We think that the deviations in the position of the shear band from [5,3] reported in [7] for large $H/R_s \gtrsim 0.6$ are due to the small system size used by that group.